The Influence of Lipid Bilayer Physicochemical Properties on Gramicidin A Conformer Preferences

John W. Patrick,[1] Roberto C. Gamez,[1] and David H. Russell[1,*]

[1]Department of Chemistry, Texas A&M University, College Station, Texas

ABSTRACT   The conformational preferences adopted by gramicidin A (GA) dimers inserted into phospholipid bilayers are reported as a function of the bilayer cholesterol content, temperature, and incubation time. Through use of vesicle capture-freeze drying methodology, GA dimers were captured in lipid bilayers and the conformational preferences of the complex were analyzed using ion mobility-mass spectrometry. Perturbations that affect the physicochemical interactions in the lipid bilayer such as cholesterol incorporation, temperature, and incubation time directly alter the conformer preferences of the complex. Regardless of bilayer cholesterol concentration, the antiparallel double helix (ADH) conformation was observed to be most abundant for GA dimers in bilayers composed of lipids with 12 to 22 carbon acyl chains. Incorporation of cholesterol into lipid bilayers yields increased bilayer thickness and rigidity, and an increased abundance of parallel double helix (PDH) and single-stranded head-to-head (SSHH) dimers were observed. Bilayers prepared using 1,2-dilauroyl-*sn*-glycero-3-phosphocholine, a lipid with 12 carbon acyl chains, yielded a nascent conformer that decreased in abundance as a function of bilayer cholesterol content. High resolution ion mobility-mass spectrometry data revealed two peaks in the ADH region suggesting that ADH populations are composed of two distinct conformers. The conformer preferences of GA dimers from 1,2-distearoyl-*sn*-glycero-3-phosphocholine bilayers were significantly different for samples incubated at 4°C vs. 60°C; increased cholesterol content yielded more PDH and SSHH at 60°C. The addition of cholesterol as well as incubating samples of 1,2-distearoyl-*sn*-glycero-3-phosphocholine at 60°C for 24–72 h yielded an increase in PDH and SSHH abundance.

INTRODUCTION

Many biological processes including peptide- or protein-lipid interactions are influenced by the identity and localization of the lipids comprising cellular membranes (1,2). Membrane lipids are polymorphic entities because of their ability to exist in several different states and structures based on a number of external variables such as temperature, pressure, and pH (3,4). It has been hypothesized for many years that changes in the physicochemical interactions in the bilayer can alter the conformer distribution of membrane proteins (5,6). Cholesterol, a major component of eukaryotic cellular membranes, serves to assist in modulating the physicochemical properties (fluidity and rigidity of the bilayer) and can also influence the enthalpy of the phase transition in lipid membranes (7,8). Understanding the relationship between lipid identity and physicochemical interactions will lead to fundamental insights of the underlying mechanisms of peptide/protein interactions within lipid bilayers. Wimley noted that "…a major bottleneck in the

development of new amphipathic membrane peptide drugs arises from our inability to describe their mechanism-of-action (MOA) in physical-chemical terms…" (9). This view underscores the necessity for an increased understanding of peptide/protein interactions, especially ion-channel formation. Here, phospholipid bilayers are used to elucidate the effect of altering lipid bilayer physicochemical properties on the conformer preferences of a well-studied gramicidin ion-channel complex, namely gramicidin A (GA).

There have been numerous reports on conformer preferences of GA, a 15-residue dimer-forming ion channel. Chen recently reported the kinetics of disassociation and conformer preferences of GA dimers using electrospray ionization-ion mobility-mass spectrometry (ESI-IM-MS), collision-induced dissociation (CID), and hydrogen/deuterium exchange (HDX)-MS (10). GA dimer ions, [2 GA + 2 Na]$^{2+}$, were observed to adopt three distinct dimeric conformers in the gas phase: the parallel double helix (PDH), antiparallel double helix (ADH), and single-stranded head-to-head dimer (SSHH). MOBCAL/molecular dynamics (MD) simulations were performed to assign representative structures to experimentally observed conformers. Solvent polarity was found to directly affect the monomerization

CrossMark

kinetics and equilibrium abundances of the dimer ions. Consistent with previous solution-based NMR studies by Cross and co-workers, ADH conformers were found to be the thermodynamically preferred species from low dielectric solutions (11). HDX and CID measurements revealed a complex of GA monomers with strong intermolecular hydrogen bonds, consistent with the arrangement of known GA conformers. Coupling IM with HDX-CID methodology provided a comprehensive view of GA self-assembly/disassembly in low dielectric solutions.

We recently described a new approach, vesicle capture-freeze-drying (VCFD) coupled to ESI-IM-MS, for studies of membrane-captured GA, which showed that the conformer preferences of GA dimers are highly sensitive to the composition of the lipid bilayer (12). The conformers of lipid bilayer bound GA dimers were shown to reflect the ensemble of conformers observed in the solution phase; however, changing the identity of the lipids comprising the bilayer resulted in a significant influence on the preferred conformations of GA dimers. Factors such as temperature, sterol incorporation, and incubation time that ultimately influence the physicochemical properties of lipid bilayers have also been reported to alter the channel activity of gramicidin complexes, but GA dimers have widely been reported to be insensitive to changes in acyl chain length of the lipids comprising the bilayer (13–15). Although physical properties of the lipids have been examined, the influence of physicochemical interactions on the assemblage of peptide/protein complexes, i.e., GA ion-channels are neither well characterized nor well understood.

Lipid bilayers possess an intrinsic phase transition temperature, T_M, above which acyl chain disorder is greatest, resulting in a liquid disordered (L_D) phase. Conversely, below T_M, lipid acyl chains are ordered (gel-like), referred to as the solid ordered (S_O) phase. Cholesterol incorporation of sufficient quantity into lipid bilayers at a temperature below T_M of a given lipid yields an additional liquid-ordered phase, L_O (16). Lipid acyl chains are fully extended in this phase, similar to the S_O phase, yet retain increased lateral mobility. Cholesterol, an amphiphilic sterol, intercalates between the lipid acyl chains on either the inner or outer leaflet of lipid bilayers yielding an increase in bilayer thickness because of increased ordering (extension) of acyl chains. The intercalation of cholesterol between lipid molecules, above or below T_M, occupies the interstitial space between lipids and stiffens or increases rigidity of the lipid bilayer. The addition of cholesterol to bilayers at temperatures below their T_M is reported to fluidize the bilayer, likely through disruption of the ordered, gel-like network of lipid acyl chains (8). The addition of cholesterol above T_M is reported to decrease lateral mobility of the lipids yielding more rigid bilayers. Changes to the physicochemical properties of lipid bilayers induced by incorporation of cholesterol will undoubtedly influence the formation of GA ion channels. Relatively little is known/understood about the assemblage of ion channels

despite their important roles in both maintaining and disrupting cellular integrity. Bilayers composed of lipids with a range of T_M values (−2 to 55°C) containing cholesterol exist as an ensemble of phases, and serve to sample the landscape of membrane environments in which ion-channels may exist. Understanding, from a lipocentric point of view, how perturbations to the physicochemical interactions of peptide-lipid assemblies affect the conformer preferences of the channel-forming dimerized peptide GA, ultimately provides further insight into the mechanics and dynamics of other, more complex ion-channel systems. Here, we use ESI-IM-MS to investigate the effects of changes in the physicochemical properties of lipid bilayers, including 1) incorporation of cholesterol, 2) phase transition temperature, and 3) incubation time, on the conformer preferences of GA dimers inserted into lipid bilayers (Fig. 1). Deviations in GA conformer preferences as a result of modified physicochemical interactions in the bilayer reveal the influence these factors exhibit on the preferred ensemble of ion-channel structures.

MATERIALS AND METHODS

GA amino acid sequence: HCO-L-Val-Gly-L-Ala-D-Leu-L-Ala-D-Val-L-Val-D-Val-L-Trp-D-Leu-L-Trp-D-Leu-L-Trp-D-Leu-L-Trp-NHCH$_2$CH$_2$OH.

Materials

Gramicidin A (Sigma-Aldrich St. Louis, MO; $\geq$90% purity) was used as received and dissolved in high-performance liquid chromatography
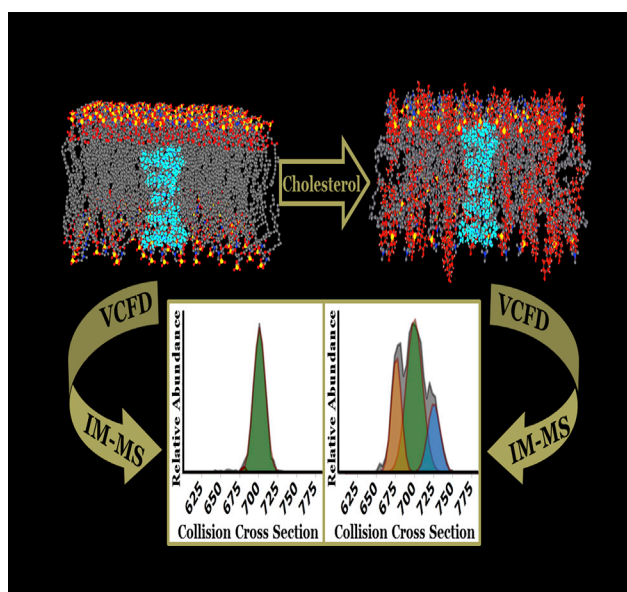

FIGURE 1 Experimental schematic for ESI-IM-MS analysis of GA-loaded bilayers. VCFD preparation is employed to analyze the effect of altering the physicochemical interactions in the bilayer on the conformational preferences of GA dimers. Depicted are bilayers without cholesterol (*left*) and with cholesterol (*right*). Perturbing the physicochemical interactions in the bilayer yields significantly different conformer preferences. To see this figure in color, go online.

grade ethanol (Sigma Aldrich) at a concentration of 1 mg/mL without further purification. Lipids were received as 10 mg/mL solutions in chloroform (Avanti Polar Lipids, Alabaster, AL) and portioned out into 500 μL aliquots containing 5 mg of lipid. High-performance liquid chromatography grade isobutanol (Alfa Aesar Ward Hill, MA) was used as received.

VCFD

Preparation of gramicidin-loaded vesicles was performed according to the VCFD method described previously (12). Briefly, samples of lipid dissolved in chloroform, and GA dissolved in ethanol, were combined, dried under nitrogen gas, and subsequently desiccated under vacuum to remove residual solvent. Samples were rehydrated to 1.0 mg/mL lipid in 18 MΩ distilled water, sonicated 30 min, and subjected to 10 freeze-thaw cycles. Samples were extruded through polycarbonate filters to yield uniform diameter lipid vesicles. Vesicle/GA solutions were allowed to equilibrate at 4°C overnight before freeze drying using liquid nitrogen and a vacuum desiccator. Before electrospray ionization (ESI), lyophilized samples were dissolved in isobutanol for analysis. All electrospray experiments were performed at room temperature. The incubation temperature of each sample differs according to the T_M of each lipid. In the case of lipids with very low T_M such as 1,2-dilauroyl-sn-glycero-3-phosphocholine (DLPC), 1-palmitoyl-2-oleoyl-sn-glycero-3-phosphocholine (POPC), and 1,2-dierucoyl-sn-glycero-3-phosphocholine (DEPC) the bilayers were prepared at room temperature, namely above their T_M. Bilayers with higher T_M, such as dipalmitoylphosphatidylcholine (DPPC) and 1,2-distearoyl-sn-glycero-3-phosphocholine (DSPC), were prepared above their T_M. DPPC bilayers were prepared at 55°C and DSPC bilayers were prepared at 60°C.

ESI-IM-MS

ESI-MS and ESI-IM-MS experiments were carried out on a Waters Synapt G2 HDMS (Waters, Milford, MA) equipped with a nano-ESI source operating at ~100°C. Spectra were acquired in positive ion mode using a 1.5–2 KV voltage applied to the capillary tips. ESI tips were manufactured in-house by a gravity-pulled method using a fused silica capillary line. Parameters for the traveling wave ion mobility cell were set at 32 V wave height and 400 m/s wave velocity.

All analyses were performed using MassLynx v4.1 software (Waters). All reported collision cross-section (CCS) values were obtained using a calibration plot from data acquired with instrument conditions identical to those used to analyze GA samples. CCS values for peptide ions, i.e., $[M + 2H]^{2+}$ ions produced by tryptic digestion of myoglobin and cytochrome C, obtained from the Clemmer database were used as calibrants (17,18). CCS calibration was performed as previously described by Ruotolo (19). Although there are discrepancies in CCS values obtained using helium versus nitrogen collision gas, reasonable agreement was observed between calibrated CCS and theoretical CCS values reported previously by Chen et al. Chen showed that ion mobility peak profiles obtained on the Synapt G2 are sensitive to instrument tuning; however, the experiments described here were all performed using instrument tuning parameters that minimize ion heating (20).

High resolution GA spectra were acquired on a Bruker Impact Q-TOF (Billerica, MA) fitted with a trapped ion mobility spectrometry (TIMS) mobility device. Calibration was performed using ESI Tune Mix (Agilent Technologies, Santa Clara, CA). Because of the location of the TIMS device in the inlet region of the mass spectrometer the gas composition is a mixture of nitrogen and ambient air yielding CCS values that are ~5% larger than those obtained on Synapt instruments.

All peak-fitting analysis was performed using Origin (OriginLab, Northampton, MA) to fit Gaussian peaks to the raw data for each arrival time distribution obtained. The number of peaks fit (n) was chosen based on the best representation of the raw data.

RESULTS

Effect of cholesterol on native GA conformer preferences

CCS profiles for GA $[2GA + 2Na]^{2+}$ ions from 100 nm vesicles containing 0–40% cholesterol formed from DLPC (12:0 PC), DPPC (16:0 PC), POPC (16:0, 18:1 PC), DEPC (22:1 PC), and DSPC (18:0 PC) prepared using the VCFD methodology are displayed in Fig. 2. The conformers shown in Fig. 2 have been labeled according to the following color scheme: purple, nascent conformer (660 Å^2); orange, PDH (675 Å^2); green, magenta, ADH (700 Å^2); and blue, SSHH (725 Å^2). Conformer preferences for samples associated with bilayers devoid of cholesterol, i.e., row one of Fig. 2, have been discussed in prior work (12). Briefly, changes in acyl chain length and extent of acyl chain unsaturation of the vesicle-forming lipids used in these studies were shown to directly alter the conformer preferences of [2 GA + 2 Na]$^{2+}$ dimer ions. GA was observed to adopt ADH conformations as the most abundant conformer in each sample. The abundances of PDH and SSHH varied depending on the lipid acyl chain length. The appearance of a nascent (fourth) GA conformer ~660 Å^2 was also observed from DLPC vesicles (Fig. 2 A) shown in purple. DSPC, a saturated lipid not explored previously, also adopts primarily ADH conformers, and PDH/SSHH abundances were observed to be dependent on the temperature of incubation as shown in Fig. 2, E and F. PDH and SSHH dimers were observed in the highest abundance from samples of POPC as well as DSPC samples incubated at 4°C.

An increase in cholesterol content of 10 mol % in the bilayer (Fig. 2, row 2), resulted in an increased abundance of PDH dimers from DLPC, DPPC, DEPC, and DSPC (60°C) samples (Fig. 2, A, B, D, and F, respectively). Abundances of PDH and SSHH dimers from POPC bilayers were observed to decrease slightly upon cholesterol incorporation. For samples of DSPC incubated at 4°C, the abundances of PDH and SSHH dimers were observed to slightly decrease. Interestingly, the nascent conformer observed from DLPC bilayers decreased in abundance with a subsequent increase in PDH abundance.

The third row in Fig. 2 displays the conformer preferences for GA from bilayers containing 40 mol % cholesterol. For all lipids except POPC and DSPC (4°C) a dramatic increase in PDH and SSHH abundance was observed. Consistent with the trends observed in rows 1 and 2, when the bilayer contained 40% cholesterol the abundance of the nascent conformer from DLPC (Fig. 2 A) decreased by ~20%, whereas PDH abundance increased to ~80%. DPPC and DSPC (60°C) displayed increases in PDH abundance of ~60% and 50%, respectively. The most significant change

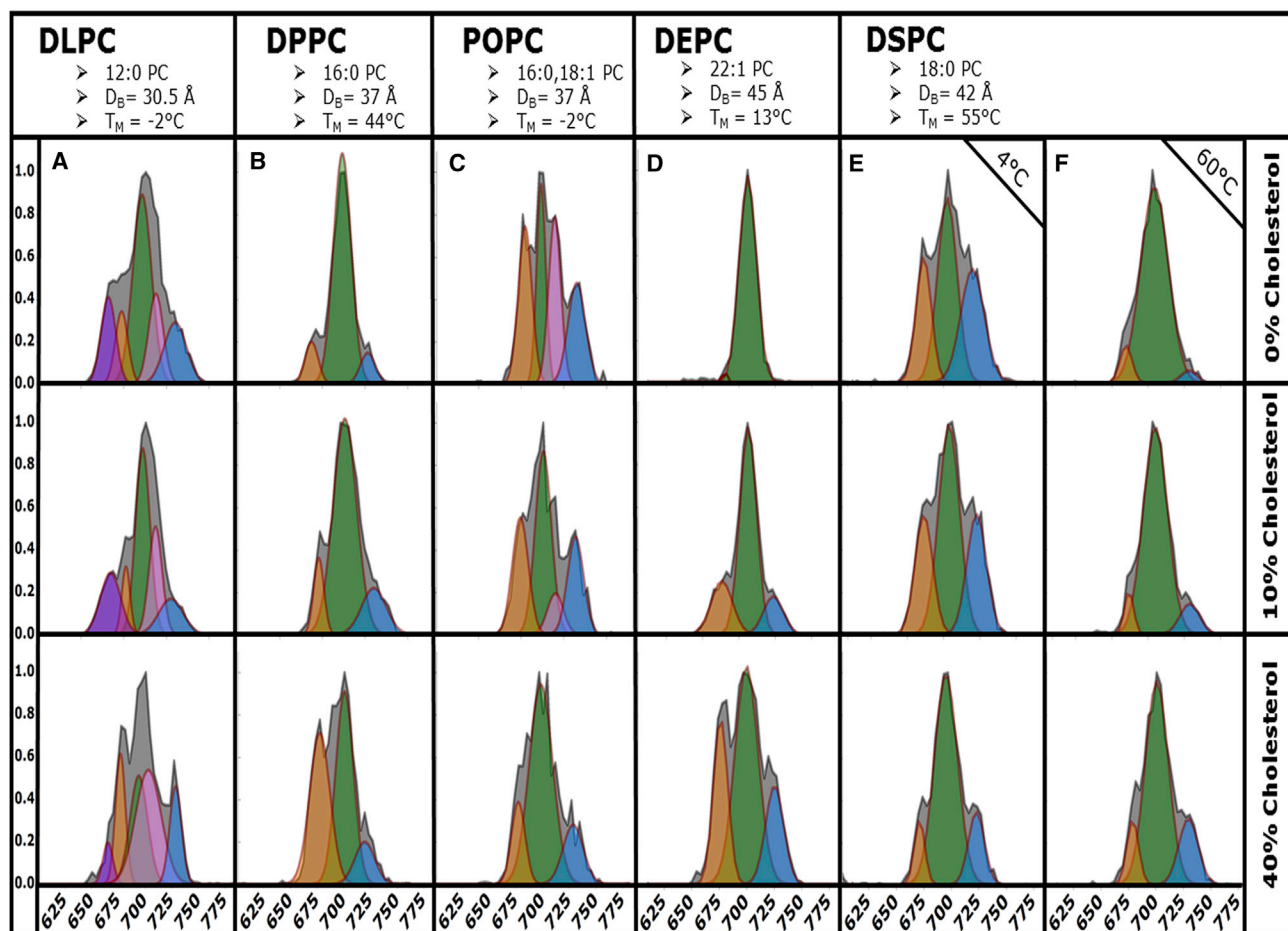FIGURE 2 CCS profiles for $[2GA + 2Na]^{2+}$ ions electrosprayed from 100 nm DLPC (*A*), DPPC (*B*), POPC (*C*), DEPC (*D*), and DSPC (*E* and *F*) vesicles containing 0–40 mol % cholesterol (*vertical*, shown at *right*) plotted as relative abundance versus CCS (Å^2). Acyl chain designations, lipid bilayer thickness (D$_B$), and gel-to-liquid phase T_M are provided for each lipid. Vesicle samples were incubated above their T_M, and DSPC was incubated at 4°C (*E*) and 60°C (*F*). Conformers have been labeled according to the following scheme: *purple*, nascent conformer (660 Å^2); *orange*, PDH (675 Å^2); *green*, *magenta*, ADH (700 Å^2); *blue*, SSHH (725 Å^2). To see this figure in color, go online.

in GA conformer preferences was observed from DEPC bilayers which, in the absence of cholesterol, displayed a nearly all-ADH arrangement, but converted to a nearly equal distribution of the three conformers upon increasing the cholesterol content to 40%. DSPC incubated at 4°C displayed a significant decrease in PDH and SSHH abundance when the cholesterol content was raised to 40% (Fig. 2, *E*, *row 3*). The conformer preferences of GA from DSPC vesicles are similar whether they are obtained from 40% cholesterol bilayers incubated at 4°C (Fig. 2 *F*, *row 1*) or with 0% cholesterol incubated at 60°C, namely the ADH conformer is the dominant conformer.

Insight into the conformational heterogeneity of GA dimer populations can be inferred from the peak widths (full width at half-maximum) in mobility space obtained from IM-MS measurements where broader peaks indicate a higher degree of heterogeneity. The number of peaks fit (*n*) was chosen based on the best representation of the raw data for each panel in Fig. 2. Peak fitting performed on experimental data where $n = 3$ resulted in poor fits for lipids DLPC and POPC. DLPC was best fit with $n = 5$, and Fig. 2 *A* shows that as cholesterol content increased, the peak widths for the nascent conformer (*purple*) narrow as the abundance of the peak decreases. Narrowing is observed for the leftmost ADH peak (*green*), whereas the second ADH peak fit (*magenta*) broadens as it increases in abundance corresponding to an increase in the cholesterol content. Additionally, the width of the PDH peak (*orange*) broadens as cholesterol content increases. PDH peak widths remained unaffected by cholesterol incorporation for other lipids examined in this study. Similarly, POPC was best fit with $n = 4$ suggesting the presence of two conformers under the broad ADH population. DPPC, DEPC, and DSPC were best fit with $n = 3$. The peak deconvolutions presented in Fig. 2 represent a mixture of $n = 3$ or 4, except in the case of DLPC, where a nascent peak was observed. Note that $n = 4$ peak fits display two ADH peaks, which have been colored green and magenta to denote the lower and

higher CCS peaks. When $n = 3$, only one ADH peak exists and thus has been fit with a green fill only. Figures displaying only $n = 3$ or $n = 4$ peak fits are included in Figs. S1 and S2 in the Supporting Material for comparison.

The most intriguing observation arises from examining ADH peak widths for DEPC and DSPC (Fig. 2, D–F). ADH peak widths (full width at half-maximum) increased from 18.43 Å^2 with no cholesterol present to 25.04 Å^2 for DEPC bilayers containing 40% cholesterol indicating an overall increase in the heterogeneity of the ADH population. This phenomenon is observed to be temperature-dependent for DSPC bilayers. ADH peak widths from DSPC bilayers (incubated at 4°C) containing 0% cholesterol were observed to increase from 20.86 Å^2 to 24.91 Å^2 with 40% cholesterol present. For DSPC bilayers containing 0% cholesterol (incubated at 60°C) ADH peak widths were observed to decrease from 29.63 Å^2 to 24.84 Å^2 with 40% cholesterol present.

Elucidation of the structure and number of ADH populations through CCS profile peak fitting and high-resolution TIMS data

Fig. 3 displays CCS profiles for [2 GA + 2 Na] $^{2+}$ ions electrosprayed from 100 nm POPC vesicles. Panels A and B display identical raw data obtained from samples prepared by VCFD methodology on a Synapt G2 HDMS that were fit with three and four peaks, respectively. The same sample was analyzed on a prototype high-resolution IMS instrument (ESI-TIMS-QTOF) (R > 100) with results shown in Fig. 3 C. Because of the differences in the composition of the drift gas environment, the CCS values obtained are inherently different between these two instruments. Regardless of CCS, the high resolution data revealed two peaks that fall within the range of the ADH region (740–760 Å^2) suggesting that ADH populations are composed of two distinct conformers. This is not surprising, as previous investigations on GA dimers using HDX revealed two ADH populations with different rates of deuterium exchange (10). Additionally, the two most populated clusters produced from MD simulations for each conformer are shown in the top right panel.

Effects of incubation at elevated temperature on conformer preferences of native GA in DSPC bilayers

Fig. 2 demonstrates that GA from DSPC bilayers experiences a significant change in the conformer preferences
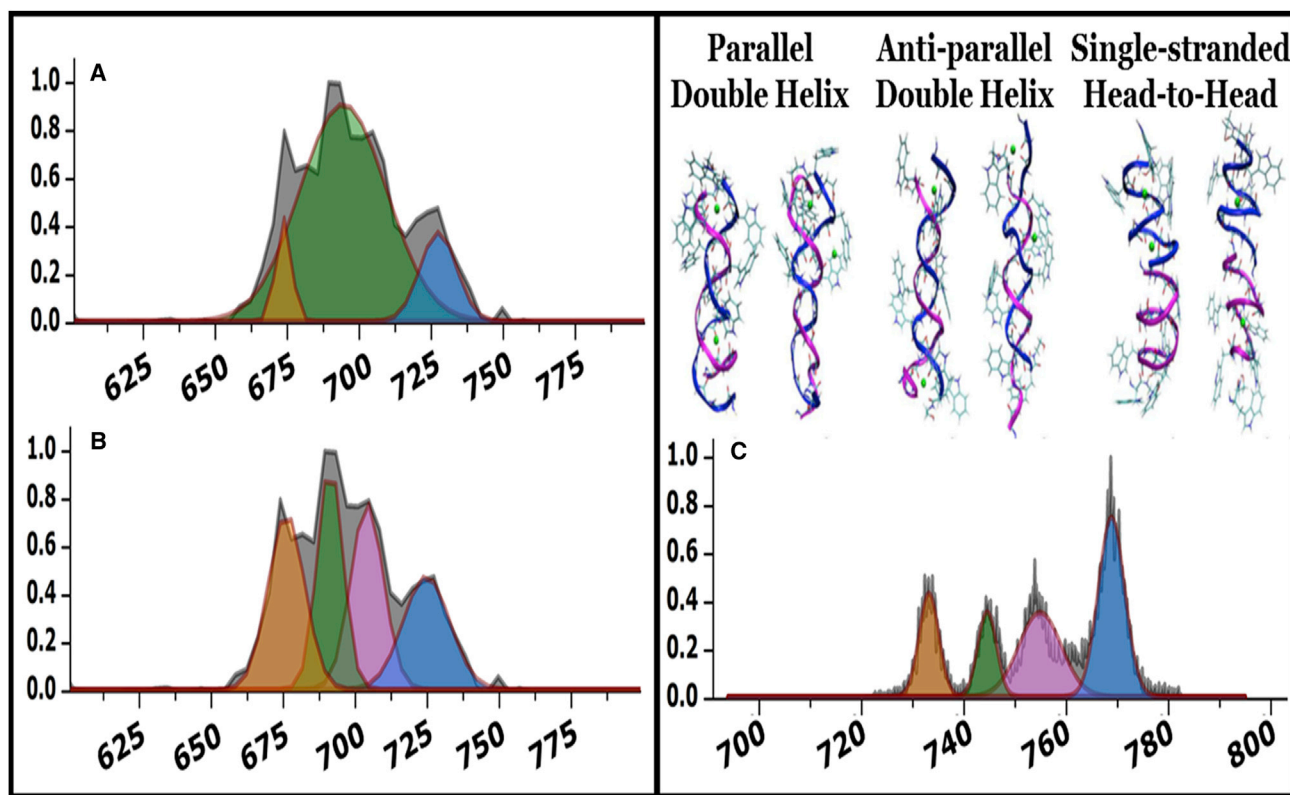

FIGURE 3 CCS profiles for [2GA + 2Na]$^{2+}$ ions electrosprayed from 100 nm POPC vesicles plotted as relative abundance versus CCS (Å^2). (A and B) Identical data obtained on a Synapt G2 (R ~25) fit using $n = 3$ peak fits (A) and $n = 4$ peak fits (B). (C) High-resolution data obtained on a prototype Bruker TIMS instrument with R > 100. Note the magenta nascent peak revealed under the ADH distribution using $n = 4$ peak-fits in panel (B) and the high-resolution TIMS instrument. MD simulations were performed previously to generate candidate structures for each population, and the two most populated structures for each conformer are shown at top right. To see this figure in color, go online.

upon increasing the incubation temperature from 4 to 60°C (Fig. 2, E and F). The effects of incubation time at elevated temperature were examined by incubating DSPC vesicles at 60°C for periods of 24, 48, and 72 h. Fig. 4 displays CCS profiles for $[2GA + 2Na]^{2+}$ ions from 100 nm DSPC vesicles containing 0–40% cholesterol incubated at 60°C for 24 (Fig. 4 A), 48 (Fig. 4 B), and 72 (Fig. 4 C) h, respectively. At all incubation times, SSHH is observed to be most abundant from bilayers containing 40% cholesterol. Fig. 4, A–C, demonstrates that as cholesterol content increases, PDH and SSHH increase in abundance after 24 h of incubation. The magnitude of this increase is greater at longer incubation times, hence, the most significant effect is observed from

72 h of incubation for bilayers containing 40% cholesterol (Fig. 4 C).

DISCUSSION

The conformer preferences, multimeric state, and biological functionality of membrane-bound peptides/proteins are sensitive to changes in physicochemical interactions in the bilayer (7,21,22). The physicochemical interactions that dictate bilayer properties such as fluidity i.e., lateral mobility of the ensemble of lipids that self-assemble to form bilayer membranes, can be perturbed through incorporation of small molecules such as cholesterol, or through
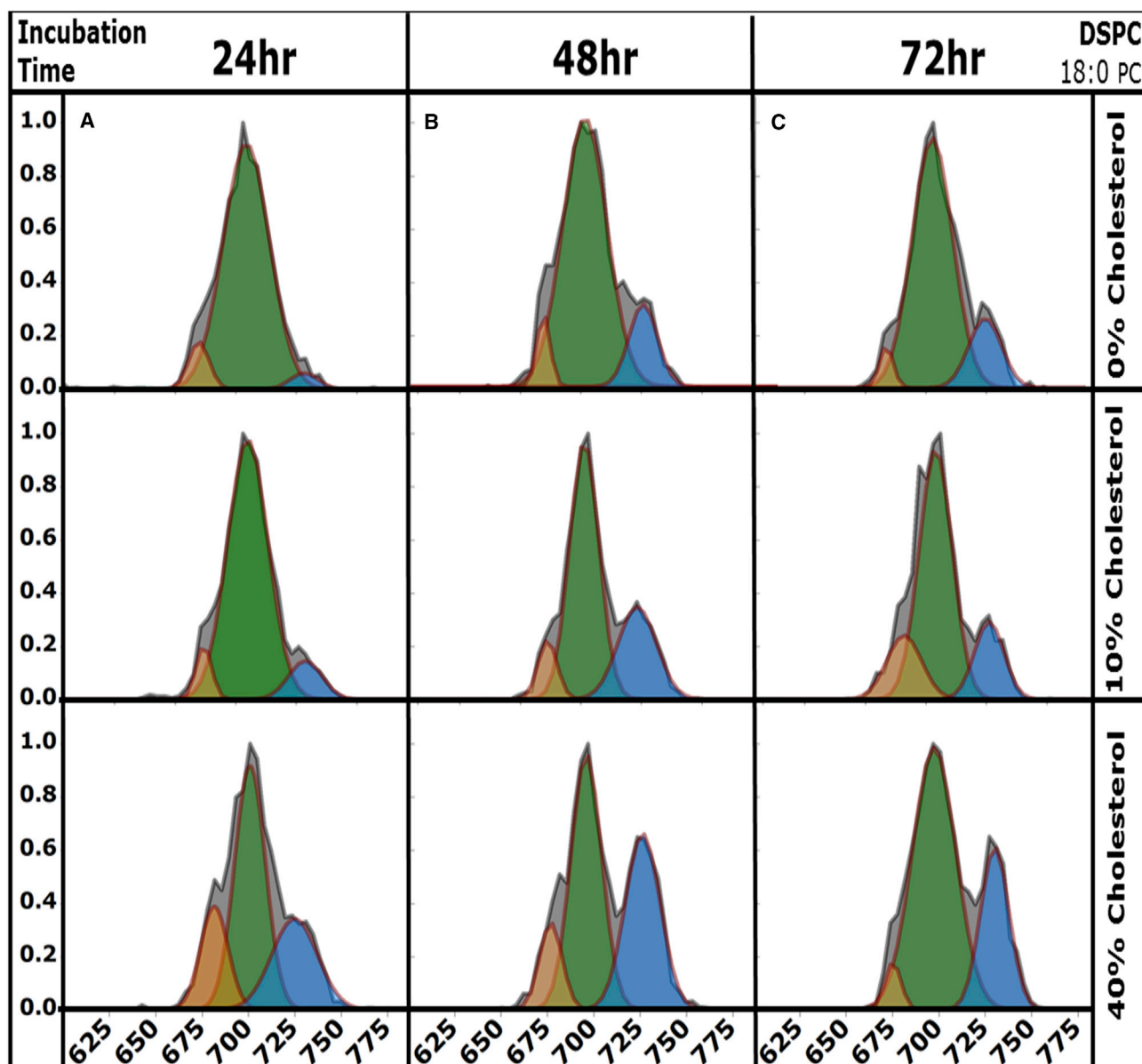

FIGURE 4 CCS profiles for $[2GA + 2Na]^{2+}$ ions electrosprayed from 100 nm DSPC vesicles containing 0%, 10%, or 40% cholesterol are plotted as relative abundance versus CCS (Å²). Samples were incubated at 60°C for 24 h (A), 48 h (B), and 72 h (C). At all incubation times, SSHH (shown in *blue*) abundance increases when 40% cholesterol is present. To see this figure in color, go online.

changes in lipid phase correlating to temperature effects (16). Herein, the conformer preferences of GA dimers captured from lipid bilayers provide insight into how perturbations of physicochemical interactions influence the ensemble of conformers observed using ESI-IM-MS.

Fig. 2 displays CCS profiles for $[2GA + 2Na]^{2+}$ ions from vesicles composed of lipids (see figure caption) incorporating 0–40 mol % cholesterol. GA dimer conformer preferences are altered, in a lipid-dependent manner, upon incorporation of cholesterol into the bilayer observed as perturbations in PDH/SSHH abundance and IMS peak widths for ADH conformers. There exists a phenomenon known as the "dual-effect" nature of cholesterol, which suggests that the influence of cholesterol on the physicochemical properties of lipid bilayers is dependent upon the temperature of the system in relation to the T_M of a given bilayer. Bilayers formed from lipids with low T_M ($-2°C$), such as DLPC and POPC (Fig. 2, A and C, respectively) possess relatively disordered lipid acyl chains at room temperature. Introduction of rigid cholesterol into fluid bilayers yields an ordering effect on lipid acyl chains, and decreases their lateral mobility. Conversely, disordering effects on acyl chains occur at room temperature if cholesterol is incorporated into bilayers with higher T_M such as DPPC, DEPC, and DSPC (Fig. 2, B, D, and F, respectively). Regardless of temperature, the addition of cholesterol is reported to increase the thickness of the hydrocarbon-rich bilayer interior.

Cholesterol has a direct influence on GA conformer preferences as shown in Fig. 2 A (DLPC). DLPC bilayers devoid of cholesterol are thin and exhibit moderate lateral acyl chain mobility at room temperature because of the low T_M. The appearance of a nascent conformer described previously, shown as the purple peak at 660 $Å^2$, is only observed from DLPC vesicles. We hypothesize that this nascent conformer arises because of a mechanical compression exerted on the complex only under conditions that exist within very thin bilayers. Upon increasing cholesterol content to 10% or 40% (Fig. 2 A, rows 2–3), a decrease in abundance of the nascent conformer was observed. This result is not unexpected; it has long been known that hydrophobic coupling between membrane proteins and acyl chains can yield changes in protein conformation (23–25). The addition of cholesterol thickens the bilayer, increases lateral lipid mobility, and relaxes positive hydrophobic mismatch and mechanical compression (26). In fact, Andersen and co-workers have reported that SSHH GA conformers are intimately related to deformations in the bilayer thickness, both contraction and expansion, that influence channel conductance through coupling of hydrophobic thicknesses between GA and acyl chains (27,28). Accordingly, an increase in bilayer thickness in combination with a decrease in the lateral mobility of acyl chains may explain why SSHH dimers were observed to be more abundant at 10% or greater cholesterol content from DLPC bilayers. Extended acyl chains would permit increased movement and thus would be more likely to adapt to accommodate the relatively wide and bulky SSHH dimer. Furthermore, broadening of ADH IMS peak widths as a function of cholesterol content indicates an increase in the heterogeneity of these populations, namely a broader ensemble of populated conformational states.

Vesicles were formed from DEPC (Fig. 2 D), which yield thicker bilayers than DLPC, to study how the effects of cholesterol are related to bilayer thickness. GA complexes associated with DEPC bilayers likely experience negative hydrophobic mismatch, i.e., dimpling of the bilayer, and have been reported to undergo structural changes (29). It was thus hypothesized that thick DEPC bilayers would exert a stretching force on GA dimers. It is not surprising that ADH dimers, hypothesized to anchor themselves on either side of the bilayer via Trp residues positioned at the interface of the solvent/bilayer regions, are the only conformers observed from DEPC vesicles (30,31). Rows 2–3 of Fig. 2 D support the hypothesis that swelling of the bilayer as a result of cholesterol incorporation may result in the disassociation/rearrangement of these anchored ADH dimers followed by subsequent association/rearrangement of PDH/SSHH. Increases in PDH and SSHH abundance upon increasing amounts of cholesterol in the bilayer (Fig. 2, A and D, rows 2 and 3) were observed from both DLPC and DEPC. We hypothesize this trend arises because of two opposing mechanisms: 1) thickening the bilayer through cholesterol incorporation promotes interconversion from either nascent (DLPC) or ADH conformers to PDH / SSHH dimers, or 2) cholesterol aids in the retention of PDH/SSHH dimer structure.

We hypothesize that changes in conformation that result from the slipping apart of GA dimers could be observed using IMS. In fact, the sensitivity of the fitted peak widths for the ADH IMS distributions to cholesterol content discussed previously suggests that there exists more than one family of ADH conformers. This hypothesis aligns directly with evidence reported by Durkin and Andersen that SSHH GA dimers can slip apart via breakage of two H-bonds between GA monomers, resulting in an increase in GA monomer bond distance of 0.16 nm (27,32). GA has been previously shown to adopt three conformer populations, and GA CCS profiles were originally fit using three total peaks; however, in some cases an improved fit was obtained by increasing the number of peaks fit from three (Fig. 3 A) to four (Fig. 3 B). Two distinct conformers exist under the broad ADH population observed ~700 $Å^2$ at low resolution (Fig. 3 A, shown in green). This result is not unexpected, as prior MD simulations from our group on GA dimers revealed that ADH exists predominantly as two populations; a smaller CCS complex represents the preferred gas-phase ADH dimer while a larger CCS structure represents partial disassociation (Fig. 3, inset). In some cases, ADH peak widths were observed to be insensitive to cholesterol incorporation (POPC, Fig. 2 C). High-resolution ion mobility data revealed that for GA from POPC, two distinct ADH

conformers (Fig. 3 C) were observed in relatively equal abundance between 730 and 770 Å^2 (shown in green and magenta). We hypothesize that narrowing of the ADH peak widths observed from bilayers formed from DSPC incubated above T_M (Fig. 2 F) as a function of cholesterol content suggests that depletion of one of these two sub-populations occurs; however, bilayers formed from POPC appear to be particularly resistant to such changes. We have demonstrated the sensitivity of ADH peak widths from DLPC, DPPC, DEPC, and DSPC (Fig. 2, A–F), to both acyl chain length and cholesterol content, thus it is reasonable to assume mechanically stretched complexes will yield a preference for the elongated ADH dimer, and vice versa. Further studies are underway using high-resolution TIMS to elucidate how the abundances of ADH sub-structures are perturbed by changes in physicochemical interactions from bilayers that are sensitive to cholesterol incorporation.

The effect of temperature and incubation time on GA conformer preferences from DSPC bilayers

The lipid bilayer in eukaryotic organisms is a heterogeneous landscape because of the diverse nature of membrane-active peptides and proteins. The integral role that temperature plays on the phase behavior of lipid bilayers, namely changes in the physicochemical interactions of the acyl chains has been understood for many years (33). Native bilayers remain at a relatively constant temperature and organisms rely on the enrichment of a number of lipids with specific physical properties, i.e., alkyl chain length and extent of unsaturation, to govern peptide- or protein-lipid physicochemical interactions. The complexity of these natural bilayers makes characterization of specific interactions between lipids and peptide or protein difficult. To further understand how changes in bilayer phase behavior affect the conformer preferences of GA complexes, the effects of varying the temperature of a well-understood monocomponent DSPC lipid bilayer were examined.

High T_M lipids provide a unique system wherein lipid bilayer phase behavior can be manipulated through temperature control of the bilayer. At low temperature, DSPC bilayers remain in the S_O (gel-like/solid ordered) phase and thus the lateral mobility of the lipids comprising the bilayer is restricted. At temperatures above the T_M of DSPC (55°C), the lipid acyl chains increase in lateral mobility yielding an L_D phase (34). An additional L_O phase exists when cholesterol is present in sufficient quantity below the T_M of a given lipid wherein lipid acyl chains are ordered as in the S_O phase yet retain increased lateral mobility. Phase behavior can be tuned because of the high T_M of DSPC to permit observations on how GA conformer preferences are affected in S_O versus L_D phases. The appearance of an L_O phase provides insight into the differences in GA conformer preferences observed when perturbing a system

that originally exists predominantly in the S_O versus L_D phases.

At 4°C, the DSPC bilayer exists in the S_O phase where lipid acyl chain lateral mobility is limited and an abundance of all three conformers—PDH, ADH, SSHH—were observed (Fig. 2 E), shown in orange, green, and blue, respectively. Introducing cholesterol (Fig. 2 E, rows 2–3), increased acyl chain lateral mobility at low temperature, likely through formation of an L_O phase, yielding a CCS profile that appears similar to DSPC incubated above T_M (Fig. 2F). This observation supports the notion that DSPC bilayers containing GA and cholesterol, when incubated above the T_M, may experience decreased lateral mobility because of the presence of cholesterol. We hypothesized that above T_M, DSPC would behave similar to DEPC wherein ADH dimers appeared to convert to PDH/SSHH as a function of cholesterol content. Nagao and co-workers demonstrated that a negative hydrophobic mismatch occurs between GA in the L_O phase DSPC bilayers, and similar trends in PDH/SSHH abundance as demonstrated from DEPC are observed in DSPC (35). Our observations from DSPC suggest that gel-like bilayers preserve conformer preferences adopted in the S_O phase, as evidenced by the increased abundances of PDH and SSHH dimers when comparing Fig. 2, E and F. Elevating the incubation temperature above T_M increases acyl chain mobility allowing rearrangement to primarily ADH dimers. DEPC, a longer acyl chain lipid (Fig. 2 D), did not adopt similar temperature-related behavior, which may be attributed to points of unsaturation in its acyl chain. Unsaturation of the acyl chains introduces disorder through the addition of kinks in the chain typically yielding bilayers with much lower T_M than their saturated-chain analogs. Upon increasing cholesterol content, above T_M, lateral mobility of the lipids are reduced such that GA conformer preferences in DSPC appeared more similar to those observed from S_O-phase bilayers despite the bilayer existing as a mixture of L_O/L_D phases. Under conditions of increased incubation temperature/time the bilayer remains relatively fluid and thus ADH, the preferred conformer, is not disrupted by perturbations of the bilayer phase.

Length of incubation on conformer preferences of GA in DSPC bilayers

Fig. 4 demonstrates that SSHH abundance at 40% cholesterol increases as a function of incubation time, indicating that over longer timescales formation of the head-to-head dimer complex becomes more favorable. This result is not entirely unexpected, as Killian and co-workers reported that incubation of a GA sample at ~70°C promotes rearrangement into SSHH conformers (36). ADH peak widths for 40% cholesterol significantly broadened after 72 h incubation when compared to 24–48 h of incubation. The broadening observed for ADH suggests that the bilayer environment is changing, after 72 h, as denoted by changes

in the abundances of ADH conformers. This argument is further supported by the disappearance of PDH dimers. The abundance of SSHH after 48 h did not change, suggesting that at higher temperature, longer timescales, and with more cholesterol present, SSHH dimers are more stable than PDH or ADH conformers. For some time it has been reported that cholesterol can aggregate in bilayers to form rafts or regions of cholesterol enrichment resembling patches on the bilayer surface (37–39). The effects observed here may result from a redistribution of cholesterol in the bilayer. SSHH formation appears to be promoted by the organizing effect on acyl chains that arise from the presence of cholesterol above T_M along with decreased lipid lateral mobility. The association of monomers embedded in either the exterior or interior leaflet has been proposed as the primary mechanism for SSHH formation (27). We hypothesize that GA monomers from DSPC bilayers, under extended incubation times in the presence of cholesterol, experience enhanced formation of head-to-head dimers because of the decrease in lipid lateral mobility promoting increased GA-GA interactions. Fig. 4 A shows that 24 h incubation is sufficient, in the presence of 10–40% cholesterol, to increase SSHH abundance. This evidence suggests that a decrease in the lateral mobility of lipids as a result of cholesterol incorporation promotes the association of GA monomers yielding an increase in SSHH abundance. Although further studies are underway to probe this phenomenon, it is evident that the conformer preferences observed for GA dimers are a result of incubation time as well as competing physicochemical interactions between cholesterol and lipid acyl chains.

CONCLUSIONS

Understanding how factors that govern the physicochemical properties of lipid bilayers affect the conformer preferences of biomolecules is a unique challenge emerging at the interface of analytical chemistry, biology, and biophysics. Herein, we successfully demonstrate the use of VCFD coupled to ESI-IM-MS to provide insight into the effects of cholesterol incorporation, incubation temperature, and incubation time on GA dimer conformer preferences associated with lipid vesicle bilayers. We have previously shown that the conformer preferences of GA dimers are dependent on the composition of the lipid bilayer with which they associate. Here, we have shown that the incorporation of cholesterol into the bilayer yields an increased abundance of SSHH dimers and increases peak widths for ADH conformers. For bilayers formed from DSPC (18:0 PC), which possess a high T_M (55°C), we observed that GA conformer preferences varied significantly upon incubation above or below the lipid's T_M. Incubation above T_M yielded a lower abundance of PDH and SSHH dimers, whereas incubation below T_M yielded an ensemble of all three GA dimer conformers. Cholesterol was observed to alter the conformer preferences of GA dimers from DSPC in a temperature-

dependent manner. Above T_M, the addition of cholesterol yielded narrowed ADH distributions and increased PDH and SSHH abundance. Conversely, below T_M the addition of cholesterol yielded decreased PDH and SSHH abundance with broader ADH populations. These results suggest that cholesterol directly affects the lateral mobility, i.e., fluidity of the lipid bilayer in a temperature-dependent manner. Increasing incubation time of a sample of DSPC, above T_M, yielded an increase in SSHH abundance as well as a broadening of the ADH dimer peak corresponding to an increase in cholesterol content in the bilayer. This study elucidates the role that temperature, cholesterol incorporation, and incubation time play on the conformer preferences of the model ion-channel GA using IM-MS. More importantly, VCFD coupled to IM-MS provides a means by which comparisons can be made to relate changes in various physicochemical interactions with the far-reaching effects these changes have on peptide/protein structural preferences.

SUPPORTING MATERIAL

Two figures are available at http://www.biophysj.org/biophysj/supplemental/S0006-3495(16)30071-6.

AUTHOR CONTRIBUTIONS

J.W.P., R.C.G., and D.H.R. designed the study. J.W.P. performed the experiments, analyzed and interpreted the data, and produced the figures. J.W.P. and D.H.R. wrote the article. The authors wish to thank Drs. Mel Park and Joshua Silveira at Bruker Corporation for their gracious use of high-resolution ion mobility instrumentation.

ACKNOWLEDGMENT

REFERENCES

1. Spector, A. A., and M. A. Yorek. 1985. Membrane lipid composition and cellular function. *J. Lipid Res.* 26:1015–1035.

2. Lundbaek, J. A. 2008. Lipid bilayer-mediated regulation of ion channel function by amphiphilic drugs. *J. Gen. Physiol.* 131:421–429.

3. Lee, A. G. 2005. How lipids and proteins interact in a membrane: a molecular approach. *Mol. Biosyst.* 1:203–212.

4. Marsh, D. 2008. Protein modulation of lipids, and vice-versa, in membranes. *Biochim. Biophys. Acta.* 1778:1545–1575.

5. Sackmann, E. 1984. Physical basis of trigger processes and membrane structures. *In* Biological Membranes. D. Chapman, editor. Academic Press, London, UK, pp. 105–143.

6. Andersen, O. S., and R. E. Koeppe, 2nd. 2007. Bilayer thickness and membrane protein function: an energetic perspective. *Annu. Rev. Biophys. Biomol. Struct.* 36:107–130.

7. Lundbaek, J. A., P. Birn, …, O. S. Andersen. 1996. Membrane stiffness and channel function. *Biochemistry.* 35:3825–3830.

8. Lundbaek, J. A., P. Birn, …, O. S. Andersen. 2004. Regulation of sodium channel function by bilayer elasticity: the importance

of hydrophobic coupling. Effects of Micelle-forming amphiphiles and cholesterol. *J. Gen. Physiol.* 123:599–621.

9. Wimley, W. C., and K. Hristova. 2011. Antimicrobial peptides: successes, challenges and unanswered questions. *J. Membr. Biol.* 239:27–34.

10. Chen, L., S. H. Chen, and D. H. Russell. 2013. An experimental study of the solvent-dependent self-assembly/disassembly and conformer preferences of gramicidin A. *Anal. Chem.* 85:7826–7833.

11. Pascal, S. M., and T. A. Cross. 1993. High-resolution structure and dynamic implications for a double-helical gramicidin A conformer. *J. Biomol. NMR.* 3:495–513.

12. Patrick, J. W., R. C. Gamez, and D. H. Russell. 2015. Elucidation of conformer preferences for a hydrophobic antimicrobial peptide by vesicle capture-freeze-drying: a preparatory method coupled to ion mobility-mass spectrometry. *Anal. Chem.* 87:578–583.

13. Wallace, B. A., W. R. Veatch, and E. R. Blout. 1981. Conformation of gramicidin A in phospholipid vesicles: circular dichroism studies of effects of ion binding, chemical modification, and lipid structure. *Biochemistry.* 20:5754–5760.

14. Greathouse, D. V., J. F. Hinton, …, R. E. Koeppe, 2nd. 1994. Gramicidin A/short-chain phospholipid dispersions: chain length dependence of gramicidin conformation and lipid organization. *Biochemistry.* 33:4291–4299.

15. Galbraith, T. P., and B. A. Wallace. 1998. Phospholipid chain length alters the equilibrium between pore and channel forms of gramicidin. *Faraday Discuss.* 111:159–164, discussion 225–246.

16. Evans, E., and D. Needham. 1987. Physical properties of surfactant bilayer membranes: thermal transitions, elasticity, rigidity, cohesion, and colloidal interactions. *J. Phys. Chem.* 91:4219–4228.

17. Hoaglund, C. S., S. J. Valentine, …, D. E. Clemmer. 1998. Three-dimensional ion mobility/TOFMS analysis of electrosprayed biomolecules. *Anal. Chem.* 70:2236–2242.

18. Henderson, S. C., S. J. Valentine, …, D. E. Clemmer. 1999. ESI/ion trap/ion mobility/time-of-flight mass spectrometry for rapid and sensitive analysis of biomolecular mixtures. *Anal. Chem.* 71:291–301.

19. Ruotolo, B. T., J. L. P. Benesch, …, C. V. Robinson. 2008. Ion mobility-mass spectrometry analysis of large protein complexes. *Nat. Protoc.* 3:1139–1152.

20. Chen, S. H., and D. H. Russell. 2015. How closely related are conformations of protein ions sampled by IM-MS to native solution structures? *J. Am. Soc. Mass Spectrom.* 26:1433–1443.

21. Brown, M. F. 1994. Modulation of rhodopsin function by properties of the membrane bilayer. *Chem. Phys. Lipids.* 73:159–180.

22. Chang, H. M., R. Reitstetter, …, R. Gruener. 1995. Attenuation of channel kinetics and conductance by cholesterol: an interpretation using structural stress as a unifying concept. *J. Membr. Biol.* 143:51–63.

23. Owicki, J. C., M. W. Springgate, and H. M. McConnell. 1978. Theoretical study of protein–lipid interactions in bilayer membranes. *Proc. Natl. Acad. Sci. USA.* 75:1616–1619.

24. Unwin, P. N., and P. D. Ennis. 1984. Two configurations of a channel-forming membrane protein. *Nature.* 307:609–613.

25. Unwin, N., C. Toyoshima, and E. Kubalek. 1988. Arrangement of the acetylcholine receptor subunits in the resting and desensitized states, determined by cryoelectron microscopy of crystallized *Torpedo* postsynaptic membranes. *J. Cell Biol.* 107:1123–1138.

26. Patra, M. 2005. Lateral pressure profiles in cholesterol-DPPC bilayers. *Eur. Biophys. J.* 35:79–88.

27. Lundbaek, J. A., and O. S. Andersen. 1999. Spring constants for channel-induced lipid bilayer deformations. Estimates using gramicidin channels. *Biophys. J.* 76:889–895.

28. Nielsen, C., M. Goulian, and O. S. Andersen. 1998. Energetics of inclusion-induced bilayer deformations. *Biophys. J.* 74:1966–1983.

29. Mobashery, N., C. Nielsen, and O. S. Andersen. 1997. The conformational preference of gramicidin channels is a function of lipid bilayer thickness. *FEBS Lett.* 412:15–20.

30. Demmers, J. A. A., E. van Duijn, …, J. A. Killian. 2001. Interfacial positioning and stability of transmembrane peptides in lipid bilayers studied by combining hydrogen/deuterium exchange and mass spectrometry. *J. Biol. Chem.* 276:34501–34508.

31. Demmers, J. A. A., J. Haverkamp, …, J. A. Killian. 2000. Electrospray ionization mass spectrometry as a tool to analyze hydrogen/deuterium exchange kinetics of transmembrane peptides in lipid bilayers. *Proc. Natl. Acad. Sci. USA.* 97:3189–3194.

32. Durkin, J. T., L. L. Providence, …, O. S. Andersen. 1993. Energetics of heterodimer formation among gramicidin analogues with an NH2-terminal addition or deletion. Consequences of missing a residue at the join in the channel. *J. Mol. Biol.* 231:1102–1121.

33. Lewis, B. A., and D. M. Engelman. 1983. Lipid bilayer thickness varies linearly with acyl chain length in fluid phosphatidylcholine vesicles. *J. Mol. Biol.* 166:211–217.

34. Smith, K. A., and J. C. Conboy. 2012. A simplified sum-frequency vibrational imaging setup used for imaging lipid bilayer arrays. *Anal. Chem.* 84:8122–8126.

35. Hiroaki, S., I. Masashi, …, H. Nagao. 2012. Molecular dynamics study of gramicidin a in lipid bilayer: structure and lateral pressure profile. *Int. J. Quantum Chem.* 112:3834–3839.

36. Killian, J. A., K. U. Prasad, …, D. W. Urry. 1988. The membrane as an environment of minimal interconversion. A circular dichroism study on the solvent dependence of the conformational behavior of gramicidin in diacylphosphatidylcholine model membranes. *Biochemistry.* 27:4848–4855.

37. Brown, D. A., and E. London. 1998. Functions of lipid rafts in biological membranes. *Annu. Rev. Cell Dev. Biol.* 14:111–136.

38. Simons, K., and G. van Meer. 1988. Lipid sorting in epithelial cells. *Biochemistry.* 27:6197–6202.

39. Simons, K., and E. Ikonen. 1997. Functional rafts in cell membranes. *Nature.* 387:569–572.

Supplemental Information

The Influence of Lipid Bilayer Physicochemical Properties on Gramicidin A Conformer Preferences

John W. Patrick, Roberto C. Gamez, and David H. Russell

The Influence of Lipid Bilayer Physicochemical Properties on Gramicidin A Conformer Preferences

John W. Patrick,[1] Roberto C. Gamez,[1] and David H. Russell[1,*]

[1]Department of Chemistry, Texas A&M University, College Station, Texas
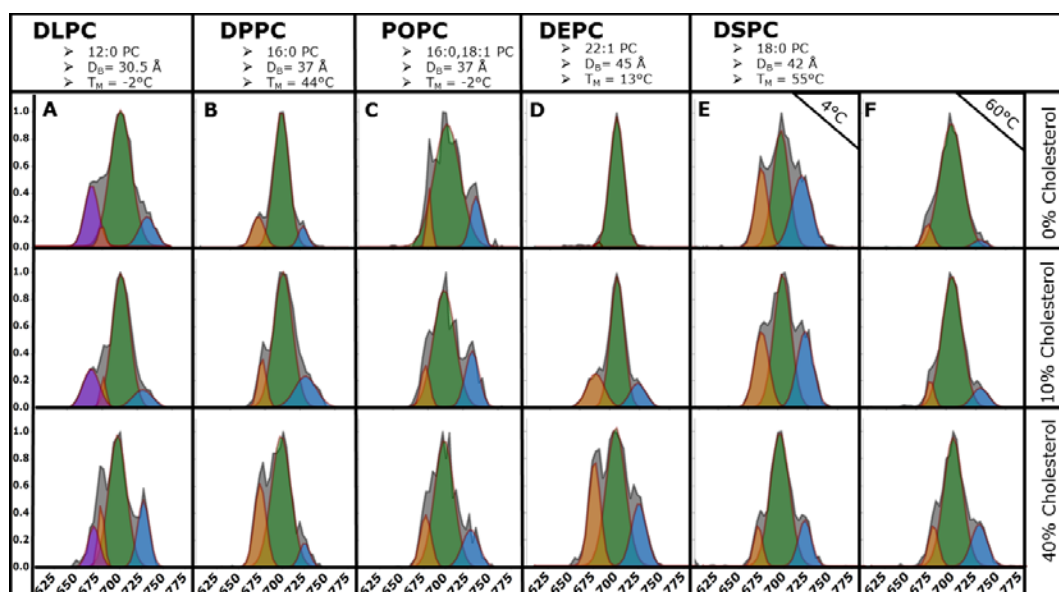
*Correspondence: russell@chem.tamu.edu

Figure S1 – CCS profiles for [2GA + 2Na]2+ ions electrosprayed from 100 nm DLPC (A), DPPC (B), POPC (C), DEPC (D), and DSPC (E-F) vesicles containing 0-40 mol% cholesterol (vertical, shown at right) plotted as relative abundance vs. CCS (Å2). Acyl chain designations, lipid bilayer thickness (DB), and gel-to-liquid phase transition temperatures (TM) are provided for each lipid. Peaks fit using n=3. Conformers have been labeled according to the following scheme: Purple – Nascent conformer (660 Å²), Orange – PDH (675 Å²), Green– ADH (700 Å²), Blue – SSHH (725 Å²).
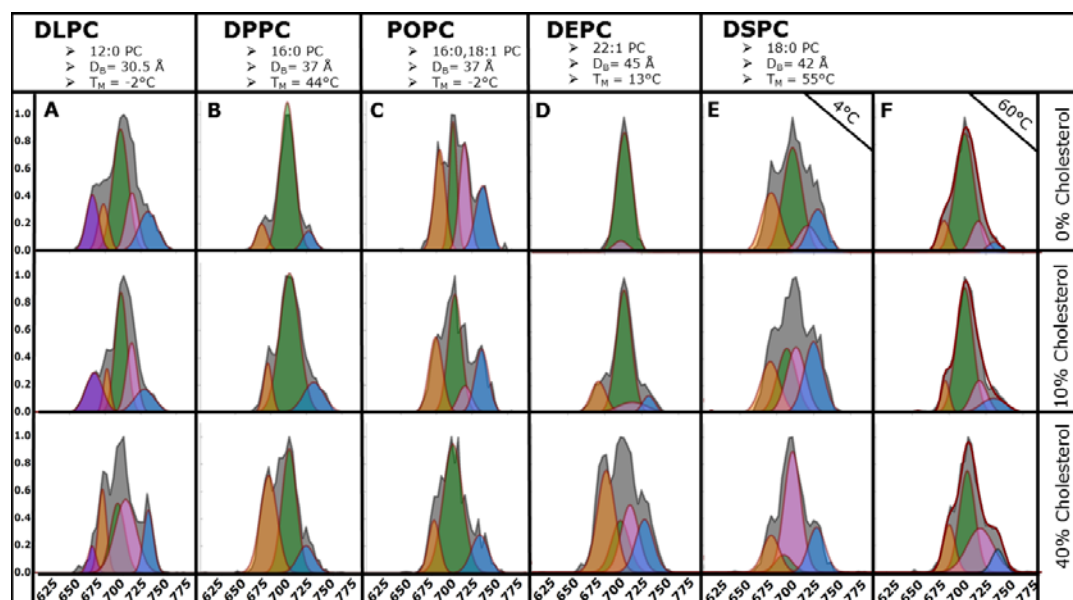

Figure S2 - CCS profiles for [2GA + 2Na]2+ ions electrosprayed from 100 nm DLPC (A), DPPC (B), POPC (C), DEPC (D), and DSPC (E-F) vesicles containing 0-40 mol% cholesterol (vertical, shown at right) plotted as relative abundance vs. CCS (Å2). Acyl chain designations, lipid bilayer

thickness (DB), and gel-to-liquid phase transition temperatures (TM) are provided for each lipid. Peaks fit using n=4. Conformers have been labeled according to the following scheme: Purple – Nascent conformer (660 Å²), Orange – PDH (675 Å²), Green, Magenta – ADH (700 Å²), Blue – SSHH (725 Å²).